Hellmann-Feynman theorem and fluctuation-correlation analysis of the Calogero-Sutherland model

Rudolf A. Römer
Institut für Physik, Technische Universität, D-09107 Chemnitz, Germany

Paul Ziesche
Max-Planck-Institut für Physik komplexer Systeme, Nöthnitzer Str. 38, D-01187 Dresden, Germany

($Revision$: 2.1; printed May 5, 2000)

Exploiting the results of the exact solution for the ground state of the one-dimensional spinless quantum gas of Fermions and impenetrable Bosons with the μ/x_{ij}^2 particle-particle interaction, the Hellmann-Feynman theorem yields mutually compensating divergences of both the kinetic and the interaction energy in the limiting case $\mu \to -1/4$. These divergences result from the peculiar behavior of both the momentum distribution (for large momenta) and the pair density (for small inter-particle separation). The available analytical pair densities for $\mu = -1/4$, 0, and 2 allow to analyze particle-number fluctuations. They are suppressed by repulsive interaction ($\mu > 0$), enhanced by attraction ($\mu < 0$), and may therefore measure the kind and strength of correlation. Other recently proposed purely quantum-kinematical measures of the correlation strength arise from the small-separation behavior of the pair density or — for Fermions — from the non-idempotency of the momentum distribution and its large-momenta behavior. They are compared with each other and with reference-free, short-range correlation-measuring ratios of the kinetic and potential energies.

71.10.-w, 05.40.-a, 71.45.Gm, 71.10.Hf, 71.10.Pm

I. INTRODUCTION

In the ground state of electron systems, it has been shown that exchange (X) due to the Pauli 'repulsion' and correlation (C) due to the Coulomb repulsion suppress particle-number fluctuations and consequently reduce the energy [1–3]. This energy reduction provides most of the 'glue' that binds atoms together to form molecules and solids [4]. Particle-number fluctuations mean that the particle number in a domain (which may be a muffin-tin sphere, a Wigner-Seitz cell, a Bader basin [5], a Daudel loge [6], a bond region between atoms in a molecule, etc.) fluctuates due to zero temperature quantum motion with a certain probability. Fulde [1] takes C_2H_2 as an example for such fluctuations. The number of valence electrons in a sphere containing a C atom fluctuates around its average value 4. Comparison of Hartree-Fock (HF) calculations for C_2H_2 with calculations which include correlation shows that the probability for finding 0, 1, 7, 8 valence electrons goes practically down to zero due to correlation. A similar fluctuation-correlation analysis is performed in Ref. [2] for several dimers and in Ref. [3] for the uniform electron gas in one, two, and three dimensions (1D, 2D, 3D). These calculations for the above mentioned narrowing of the particle-number distribution need the pair density (PD) $n(\vec{r}_1, \vec{r}_2)$ and this narrowing is used to derive from the PD a quantum-kinematical measure for the correlation strength [1]. Correlation and its strength is furthermore characterized by the small-separation (or on-top) behavior of the PD. The spherically averaged on-top curvature of the spin-parallel PD may serve as a local correlation measure [7] and from the topological analysis of the intracule PD a short-range correlation strength is defined [8]. In addition to these PD based quantities the concept of a correlation 'entropy' has been developed for Fermi systems [9–12] (in Ref. [11] the term Jaynes entropy is used). It is based on the correlation induced non-idempotency of the correlated one-particle density matrix (1PDM) $\gamma(\vec{r};\vec{r}')$. All these correlation measures intend to make the qualitative terms 'weak and strong correlation' quantitatively precise. For a survey on such measures and on relations between correlation, fluctuation, and localization see Ref. [13] and references cited therein. Note that strong correlation means extreme narrowing which is usually described as electron localization. The recent fluctuation-correlation analysis has an antecedent in Ref. [14], where fluctuation and correlation of electrons in molecules have been studied with the conclusion that all measures of the spatial localization of an electron are determined by the corresponding Fermi hole of the parallel-spin PD. For a summary of this work we refer the reader to Ref. [5]. Therein also the topological analysis of the density $\rho(\vec{r})$ has been developed which allows to identify (visualize) local groups of electrons (like atomic shells, molecular bonds, lone electron pairs, π-electron subsystems). An alternative to this density-based analysis is the PD based method of an 'electron localization function' [15]. What can be derived when the PD is known is summarized in Ref. [16], where also references are given for the comparison of calculated PDs with PDs determined from experiment (X-ray or electron scattering) via the dynamic structure factor.

Correlated 1PDM and correlated PD need correlated many-body wave functions (beyond the HF caricature), which in quantum chemistry [17,18] are traditionally obtained from configuration interaction (CI), coupled cluster (CC), Møller-Plesset, quantum Monte Carlo calculations or recently from the contracted-Schrödinger-equation method [19] (used in conjunction with a certain generation of higher-order reduced density matrices from the 2PDM via reconstruction and decoupling) or the incremental method [20] which successfully applies the accurate standard quantum-chemical methods CI and CC to extended non-metallic systems. All these procedures involve certain approximations or have restricted applicability. So the existence of non-trivial *exactly solvable models* which can provide 1PDM and PD should be of much interest for the above mentioned correlation, fluctuation, and localization analysis. The system which is of paramount importance for quantum chemistry and solid state theory but unfortunately cannot be solved exactly is the 3D electron gas with the Coulomb repulsion $\epsilon^2/|\vec{r}_{12}|$ between its particles [21]. All of its properties (like energy, momentum distribution, quasi-particle weight z_{F}, PD, static structure factor, and the more general dynamic structure factor, which contains the plasmon dispersion and damping as well as via the fluctuation-dissipation theorem the dynamical screening) depend on the dimensionless density parameter $r_s = r_0/a_{\mathrm{B}}$, where r_0 is the radius of the Wigner-Seitz sphere containing in average one electron and $a_{\mathrm{B}} = \hbar^2/m\epsilon^2$ is the Bohr radius which is characteristic for all electron systems. In the electron gas model at critical values of r_s the zero-temperature quantum phase transitions from an unpolarized gas to a polarized fluid and on to a polarized Wigner lattice appear [22]. In the following the electron gas often serves as a reference system for comparison.

In the present paper, we apply the above mentioned fluctuation-correlation analysis to the exactly solvable Calogero-Sutherland (CS) model [23]. The CS model is a model of long-range-interacting spinless particles in 1D and has been solved exactly by means of the Bethe-Ansatz technique [23,24]. The solution is valid for both fermionic and bosonic particle symmetry. Here we will mostly concentrate on the Fermi systems. Furthermore, the model can be shown to be the universal quantum model underlying the dynamical interpretation of random matrix theory [25,26]. This latter connection has been used to also compute several correlation functions exactly at three special values of the interaction strength, among them the 1PDM and the PD [23]. Thus although the information is restricted to the 1D case, the model nevertheless is ideally suited for testing the fluctuation-correlation measures discussed above.

We shall consider the ground state properties of the CS model [23]. The interaction is pairwise inversely proportional to the distance $x_{ij} = |x_i - x_j|$ of two particles with interaction strength μ, *i.e.*, μ/x_{ij}^2. The interaction strength $\mu \geq -1/4$ is occasionally parametrized as $\mu = \lambda(\lambda-1)$ with a parameter $\lambda = 1/2+\sqrt{1/4+\mu} \geq 1/2$. We shall mostly use the parameterization $\nu = \sqrt{1/4+\mu}$, such that $\mu = \nu^2 - 1/4$ and $\lambda = 1/2 + \nu$. In the thermodynamic limit we assume constant density $\rho(x) = n$, so the CS-ground state has only two parameters, ν and n. The $1/x_{ij}^2$ interaction has the peculiarity not to possess a natural length such as the Bohr radius a_{B} of the Coulomb interaction, it has no length scale per construction. Therefore it is a model showing critical behavior, which can be discussed in terms of universality classes and their conformal anomalies [27–30]. This beauty of the $1/x_{ij}^2$ interaction shows up also in the analytical Bethe-Ansatz solutions [23,31–35] and the explicit knowledge of the correlated many-body wave functions [23,36]. From the Bethe-Ansatz technique the complete energy spectrum and in particular the ground state energy per particle as a function of the interaction strength parameter ν is available [23]. We show that its kinetic and interaction 'components' can be deduced with the help of a theorem due to Schrödinger, Born, Fock, Güttinger, but usually referred to as Hellmann-Feynman theorem [37]. Surprisingly, when the interaction strength parameter ν approaches its limiting value 0, both the kinetic and the interaction energy diverge in such a way that they compensate each other leaving the total energy finite. As we outline in the following, these divergences result from the peculiar behavior of the 1PDM and the PD for $\nu \to 0$ and are related to the "fall-into-the-origin" already mentioned in Ref. [38].

For $\nu = 0, 1/2$, and $3/2$ — corresponding to $\mu = -1/4, 0$ and 2 or $\lambda = 1/2, 1$, and 2 — it has been shown [23] that the square of the ground state wave function is intimately related to the eigenvalue distribution of random matrices of the Gaussian orthogonal ensemble, the Gaussian unitary ensemble, and the Gaussian symplectic ensemble, respectively. Using this connection, Sutherland had shown how to construct the 1PDM and the PD using integral relations of random matrix theory. The resulting formulas reduce the problem, say for the 1PDM, from the evaluation of a high-dimensional integral to the computation of a determinant of a matrix [24]. From the 1PDM $\gamma(x-x')$, the momentum distributions n_κ for the three special values of μ follow via Fourier transform. Due to correlation the latter quantities are non-idempotent. They determine the mentioned correlation 'entropy' per particle $s = -\sum_\kappa n_\kappa \ln n_\kappa / \sum_\kappa n_\kappa$. Also the PD $n(x_{12})$ is available from the correlated many-body wave function. This allows us to calculate the fluctuation ΔN_X of the particle-number around its mean value $N_X = nX$ in any piece (domain) X of the x-axis. Comparing this variance of the particle-number distribution $P_X(N)$ for the cases 'no correlation' ($\nu = 1/2$ or HF approximation) and 'correlation' shows the above mentioned narrowing for repulsion ($\nu > 1/2$) in a smaller ΔN_X. For attraction ($\nu < 1/2$) a broadening with a larger ΔN_X appears.

The availability of exact solutions for certain values of the interaction strength reminds of a similar situation for the Hooke's law model, where two electrons with Coulomb repulsion are bound by a harmonic oscillator potential. In this case exact (correlated) wave functions are known for certain values of the force constant (or equivalently of the interaction strength) [39]. Within this spirit also two electrons or an electron-positron pair in a magnetic field can be treated [40,41].

In Section II, we introduce the CS model, define the kinematical quantities used throughout the text, and present the Hellmann-Feynman theorem. Section III is devoted to the thermodynamic limit. In Section IV, after presenting the HF approximation, we discuss first qualitatively and then analytically the influences of the CS interaction on 1PDM and PD. In particular, we show that the above mentioned divergences in kinetic and potential energies are caused by a peculiar behavior of the PD $n(x_{ij})$ for *small inter-particle separations* $x_{ij} \ll k_{\mathrm{F}}^{-1}$ and of the momentum distribution n_κ for *large momenta* $k \gg k_{\mathrm{F}}$ or $\kappa \equiv k/k_{\mathrm{F}} \gg 1$. In Section V we then apply the mentioned fluctuation-correlation measures to the CS model. Section VI is devoted to details of the numerics and in Section VII we discuss extensions of our approach to impenetrable bosons and lattice gases. We conclude in Section VIII with a discussion of our results.

II. THE SYSTEM AND ITS GROUND STATE

A. Hamiltonian, energies, and quantum kinematical quantities

The Hamiltonian of the CS model is $\hat{H} = \hat{T} + \hat{V}$ with

$$\hat{T} = \sum_i^N \frac{1}{2} p_i^2 \quad , \quad \hat{V} = \sum_i^N v_{\mathrm{ext}}(x_i) + \sum_{i<j}^N \frac{\mu}{x_{ij}^2} \; , \tag{1}$$

with $p_i^2 = -\partial^2/\partial x_i^2$, and N equal to the number of particles. We assume the system to be confined to the length L by an external potential $v_{\mathrm{ext}}(x)$, *e.g.*, a box or harmonic oscillator potential. In the following we alternatively assume periodic boundary conditions with $v_{\mathrm{ext}}(x) = 0$ and a density in the k space described by $L\Delta k/(2\pi) = 1$. The average particle density is $n = N/L$. Furthermore, it follows from dimensional reasons that all energies for the Hamiltonian (1) are proportional to n^2 and all lengths are measured in units of $1/n$ and all wave numbers in units of n (thus $k_{\mathrm{F}} \sim n$) [23].

We denote the ground state energy and its kinetic and potential 'components' by $E_N = \langle \hat{H} \rangle$, $T_N = \langle \hat{T} \rangle$, and $V_N = \langle \hat{V} \rangle$, respectively. Then $E_N = T_N + V_N$ and the corresponding energies per particle are $e_N = E_N/N$, $t_N = T_N/N$, $v_N = V_N/N$ with $e_N = t_N + v_N$. Let further $\Phi(x_1, \ldots, x_N)$ be the antisymmetric ground state wave function, normalized according to

$$\int \frac{dx_1 \ldots dx_N}{N!} |\Phi(x_1, \ldots, x_N)|^2 = 1 \; , \tag{2}$$

where each N-particle configuration is counted only once. Then the 1PDM is given as

$$\gamma_N(x; x') = \int \frac{dx_2 \ldots dx_N}{(N-1)!} \times \Phi(x, x_2, \ldots, x_N) \Phi^*(x', x_2, \ldots, x_N), \tag{3}$$

and the PD is

$$n_N(x_1, x_2) = \int \frac{dx_3 \ldots dx_N}{(N-2)!} |\Phi(x_1, x_2, x_3 \ldots, x_N)|^2 \; . \tag{4}$$

The PD describes the XC hole, vanishing for zero separation and approaching the Hartree product $\rho_N(x_1)\rho_N(x_2)$ for large separations. This PD is normalized as $\int dx_1 \int dx_2 \; n_N(x_1, x_2) = N(N-1)$. For the XC hole or cumulant PD $w_N(x_1, x_2) \equiv \rho_N(x_1)\rho_N(x_2) - n_N(x_1, x_2)$ this means

$$\int dx_1 \int dx_2 \; w_N(x_1, x_2) = N. \tag{5}$$

So the cumulant PD $w_N(x_1, x_2)$ is size-extensively normalized. We note that the particle density follows either from $\rho_N(x) = \gamma_N(x; x)$ or from $\rho_N(x_1) = \int dx_2 \; w_N(x_1, x_2)$, of course with the property $\int dx \; \rho_N(x) = N$.

Furthermore with the abbreviation $y = k_{\mathrm{F}} x$ — for spinless particles in 1D the Fermi wave number is $k_{\mathrm{F}} = \pi n$ [23], with spin it would be $k_{\mathrm{F}} = \pi n/2$ — and with the *dimensionless functions* $f_N(y; y')$ hermitian, $g_N(y, y')$ non-negative, and $h_N(y_1, y_2) \equiv f_N(y_1; y_1) f_N(y_2; y_2) - g_N(y_1, y_2)$, we can write for the 1PDM

$$\gamma_N(x; x') = n \; f_N(y; y'), \tag{6}$$

for the PD

$$n_N(x_1, x_2) = n^2 \; g_N(y_1, y_2), \tag{7}$$

and for the cumulant PD we have

$$w_N(x_1, x_2) = n^2 \; h_N(y_1, y_2). \tag{8}$$

The dimensionless cumulant PD is thus $h_N = 1 - g_N$ and normalized as

$$\frac{1}{N} \int \frac{dy_1}{\pi} \frac{dy_2}{\pi} \; h_N(y_1, y_2) = 1, \tag{9}$$

which follows from Eq. (5). With these dimensionless 1PDM and PD and with the Fermi energy $\epsilon_{\mathrm{F}} = k_{\mathrm{F}}^2/2$ the energies t_N and v_N are given by

$$t_N = \frac{1}{N}\int \frac{dy}{\pi}\left[-\frac{\partial^2}{\partial y^2} f_N(y;y')\right]_{y'=y} \epsilon_{\rm F} \qquad (10a)$$

and

$$v_N = \frac{1}{N}\int \frac{dy_1}{\pi}\frac{dy_2}{\pi} g_N(y_1,y_2)\frac{\mu}{y_{12}^2}\epsilon_{\rm F} \qquad (10b)$$

Therefore $t_N/\epsilon_{\rm F}$, $v_N/\epsilon_{\rm F}$ and $e_N/\epsilon_{\rm F}$ are functions of μ and N. The latter dependence disappears for the thermodynamic limit as shown in Section III.

B. The Hellmann-Feynman and the virial theorem

If e_N is known as a function of μ, then t_N and v_N can be obtained from the (Schrödinger-Born-Fock-Güttinger-) Hellmann-Feynman theorem [37] without knowing the quantum-kinematical quantities $f_N(y;y')$ and $g_N(y_1,y_2)$. This theorem says

$$\frac{\partial E_N}{\partial \mu} = \left\langle \frac{\partial \hat{H}}{\partial \mu}\right\rangle \qquad (11)$$

which for (1) gives

$$v_N = \mu \frac{\partial e_N}{\partial \mu}. \qquad (12)$$

Consequently, we have

$$t_N = \left(1-\mu\frac{\partial}{\partial \mu}\right) e_N \qquad (13)$$

and also

$$\frac{\partial}{\partial \mu} t_N = -\mu \frac{\partial}{\partial \mu}\left(\frac{1}{\mu} v_N\right) . \qquad (14)$$

Thus — with Eq. (10) in mind — the Hellmann-Feynman relation (11) for the $1/x_{ij}^2$ model establishes an integral relation between the dimensionless 1PDM f_N on the l.h.s. and the dimensionless PD g_N on the r.h.s. of Eq. (14).

Another interesting property of the $1/x_{ij}^2$ interaction is that the L or n dependence of e_N can be concluded from the virial theorem

$$2t_N + 2v_N = -L\frac{\partial e_N}{\partial L} . \qquad (15)$$

The factors 2 on the l.h.s. result from the powers of p_i in $\hat{T}$ and of $1/x_{ij}$ in $\hat{V}$. For the $1/x_{ij}$ interaction the l.h.s. would read $2t_N + v_N$. Eq. (15) means $e_N \sim L^{-2}$ or $e_N \sim n^2$, as discussed above by dimensional scaling.

III. THERMODYNAMIC LIMIT

We wish to study the thermodynamic limit with $N \to \infty$ and $L \to \infty$ such that $n = N/L = $ const. The resulting extended system has only two parameters, the (dimensionless) interaction strength parameter ν and the Fermi wave number $k_{\rm F}$. So $t/\epsilon_{\rm F}$, $v/\epsilon_{\rm F}$, and $e/\epsilon_{\rm F}$ become functions of ν only. The thermodynamic limit makes furthermore the 1PDM and the PD to depend only on $k_{\rm F}x_{12} = y_{12}$ (homogeneity, isotropy). The dimensionless functions f_N, g_N, and h_N then take the forms $f(y_{12})$, $g(y_{12})$, and $h(y_{12}) = 1-g(y_{12})$, respectively, with $f(0) = 1$ (uniform density) and $g(0) = 0$ or equivalently $h(0) = 1$. These functions have ν as the only parameter. This differs from the electron gas, where the additional parameter $r_s = r_0/a_{\rm B}$ combines for dimensional reasons the interaction strength ϵ^2 with the density $n = 3/(4\pi r_0^3)$, $1/(\pi r_0^2)$, and $1/(2r_0)$ for 3D, 2D, and 1D models, respectively.

Due to the homogeneity and isotropy, the eigenfunctions (or natural orbitals) of the 1PDM $\gamma(x-x') = nf(y)$ become simply plane waves $\varphi_k^0(x) = {\rm e}^{{\rm i}kx}/L$, such that

$$\begin{aligned}\gamma(x-x') &= \sum_\kappa \frac{1}{L} n_\kappa e^{{\rm i}\kappa k_{\rm F}\cdot(x-x')}\\ &= n\int_0^\infty d\kappa\; n_\kappa \cos\kappa y\\ &\equiv n\; f(y),\end{aligned} \qquad (16)$$

where n_κ is the momentum distribution, $\kappa = k/k_{\rm F}$, and $y = k_{\rm F}|x-x'|$.

For $\nu = 1/2$ (ideal spinless 1D Fermi gas) the Pauli principle leads in the reciprocal space to the Fermi ice block $n_\kappa^0 = \theta(1-|\kappa|)$ and in the direct space to the ideal X hole $g^0(y) = 1-[f^0(y)]^2$ with the dimensionless 1PDM $f^0(y) = (\sin y)/y$ following from Eq. (16) and with its on-top behavior $g^0(y) \to y^2/3$. The energy per particle is $e_0 = \epsilon_{\rm F}/3 = k_{\rm F}^2/6$, and because of $k_{\rm F} \sim n$ it obeys the virial theorem (15).

In general, with $\gamma(0) = n$, the momentum distribution n_κ is normalized as $\sum_\kappa n_\kappa = N$ or

$$\int_0^\infty d\kappa\; n_\kappa = 1 . \qquad (17)$$

The kinetic energy per particle is according to Eq. (10a)

$$t = 6\int_0^\infty d\kappa\; n_\kappa \frac{\kappa^2}{2} e_0 . \qquad (18)$$

n_κ is a function of $|\kappa|$ and ν, so t/e_0 is a function of ν only with $t = e_0$ for $\nu = 1/2$.

The corresponding expressions for the PD $g(y)$ are according to Eq. (9)

$$2\int_0^\infty \frac{dy}{\pi}\; h(y) = 1,\;\; h(y) = 1-g(y) \qquad (19)$$

and for the interaction energy per particle according to Eq. (10b)

$$v = 6\int_0^\infty \frac{dy}{\pi}\; g(y)\frac{\mu}{y^2}e_0\ . \tag{20}$$

$g(y)$ is a function of y and ν, so v/e_0 is a function of ν only. With t and v follows the integral relation

$$\int_0^\infty d\kappa\ \frac{\kappa^2}{2}\frac{\partial n_\kappa}{\partial\mu} = -\int_0^\infty \frac{dy}{\pi}\ \frac{\mu}{y^2}\frac{\partial g(y)}{\partial\mu} \tag{21}$$

as a consequence of the Hellmann-Feynman theorem expressed in Eq. (14). Correlation via $\nu \neq 1/2$ deforms the X hole and the Fermi ice block as shown in Figs. 1 and 2 in such a way that Eq. (21) is maintained. A similar relation for the electron gas model (with $k_{\rm F}^3 = 3\pi^2 n$) has been used for a qualitative discussion of how n_κ and $g(k_{\rm F}r_{12})$ mutually depend on the parameter r_s [42].

IV. HARTREE-FOCK APPROXIMATION AND CORRELATION BEYOND IT

A. Hartree-Fock approximation

The simplest approximation for the quantities n_κ, $g(y)$, t, and v is obtained from the HF approach. In this case the ground state wave function $\Phi_{\rm HF}(\cdots)$ is a single Slater determinant of one-particle wave functions, which are — for an extended system — simply plane waves $\varphi_k^0(x)$ as for the ideal 1D Fermi gas. Thus the momentum distribution in Eq. (18) and the PD in Eq. (20) are to be replaced by their 'ideal' expressions n_κ^0 and $g^0(y)$, respectively. Consequently, we find $t_{\rm HF} = e_0$ and $v_{\rm HF} = 2\mu e_0$ and thus $e_{\rm HF} = (1+2\mu)\, e_0$, as shown in Fig. 3. Here the identity (A5) has been used. The total HF energy $e_{\rm HF}$ also obeys the Hellmann-Feynman theorem (13) and the virial theorem (15).

B. Qualitative discussion of correlation

Due to correlation the true ground state energy per particle, e, is below the HF energy $e_{\rm HF}$ and the true ground state wave function $\Phi(\cdots)$ is no longer a single Slater determinant. Note that the definition of the term 'correlation' needs a reasonable reference state, which is $\Phi_{\rm HF}(\cdots)$ in our case. So, correlation causes a negative correlation energy $e_{\rm corr} = e - e_{\rm HF} < 0$, namely through redistributions of $g^0(y)$ and n_κ^0 which are shown in Figs. 1 and 2 and described in the following.

As we show in Fig. 1, correlation modifies the X hole of the unperturbed PD. Especially the correlation induced changes for small y are of interest, because the interaction μ/y^2 is there largest. The on-top behavior of the uncorrelated X hole ($\nu = 1/2$ or HF) is described by $g^0(y) = y^2/3 + \ldots$. In its correlated counterpart with a ν-dependent exponent and ν-dependent coefficients (see Appendix B)

$$g(y) = Ay^\alpha\left(1 + a_1 y + a_2 y^2 + \cdots\right),$$
$$\alpha = 1 + 2\nu, \quad \nu = \sqrt{\frac{1}{4} + \mu}, \tag{22}$$

correlation for $\nu \neq 1/2$ shows up in $\alpha \neq 2$ and $A \neq 1/3$. More precisely, repulsive particle interaction ($\nu > 1/2$) supports the Pauli 'repulsion', so the X hole is broadened (through increasing α and decreasing A), but attractive particle interaction ($\nu < 1/2$) fights against (or competes with) the Pauli 'repulsion', so the X hole is narrowed (through decreasing α and increasing A) as shown in Fig. 1 and Table I. This X hole narrowing (for $\nu < 1/2$) or broadening (for $\nu > 1/2$) makes

$$6\int_0^\infty \frac{dy}{\pi}\ \frac{g(y)}{y^2} = 1 + \frac{1}{2\nu} \gtrless 2 \quad \text{for} \quad \nu \lessgtr \frac{1}{2}. \tag{23}$$

The equation follows from Eq. (20) together with the Hellmann-Feynman theorem (11). Thus $v < v_{\rm HF} = 2\mu e_0$ for $\nu \neq 1/2$ as shown in Fig. 3. Below in Eq. (39) of Section V A, we will see that this PD narrowing/broadening is accompanied by enhanced particle-number fluctuations for attraction ($\nu < 1/2$) and by suppressed ones for repulsion ($\nu > 1/2$), respectively. Note the difference against the electron gas model, where only repulsion is present with suppressed particle-number fluctuations, where $g(0) = g_{\uparrow\downarrow}(0) \neq 0$, and the PD for parallel-spin electrons is zero for vanishing separation and behaves as $g_{\uparrow\uparrow}(y) = C_{\uparrow\uparrow}y^2 + \ldots$ for small separation y. This curvature coefficient $C_{\uparrow\uparrow}$ increases with increasing r_s (= increasing correlation), but the exponent of y does not change with r_s.

While in the HF approximation the PD follows from the 1PDM according to

$$n_{\rm HF}(x_{12}) = n^2 - |\gamma_{\rm HF}(x_{12})|^2\ , \tag{24}$$

correlation causes not only the change from the idempotent $\gamma_{\rm HF}(x_{12})$ to the non-idempotent $\gamma(x_{12})$ but also the appearance of an additional (non-reducible) term $u(x_{12})$ in

$$n(x_{12}) = n^2 - |\gamma(x_{12})|^2 - u(x_{12})\ . \tag{25}$$

This is the first step of the cumulant expansion [43]. Its non-reducible term $u(x_{12})$ is normalized as

$$\frac{2}{n}\int_0^\infty dx_{12}\ u(x_{12}) = c(2)\ , \tag{26}$$

where

$$
\begin{aligned}
c(2) &= 1 - \frac{2}{n}\int_0^\infty dx_{12}\ |\gamma(x_{12})|^2 \\
&= 1 - 2\int_0^\infty \frac{dy}{\pi}\ |f(y)|^2 \\
&= 1 - \int_0^\infty d\kappa\ (n_\kappa)^2 \\
&\geq 0
\end{aligned} \tag{27}
$$

is referred to as second-order non-idempotency of the 1PDM. For $\nu = 1/2$ or for the HF approximation it is $c(2) = 0$. The correlation induced non-idempotency of the 1PDM $\gamma(x_{12})$ or equivalently of the momentum distribution n_κ makes $c(2) > 0$ and let $c(2)$ increase with increasing $|\nu - 1/2|$.

This correlation induced non-idempotency means physically: Correlation excites particles and holes. This is seen in the momentum distribution n_κ as correlation tails for particles with $n_\kappa > 0$ for $|\kappa| > 1$ and for holes with $1 - n_\kappa > 0$ for $|\kappa| < 1$. In Fig. 2, we show how correlation thaws the Fermi ice block $n^0_\kappa = \theta(1 - |\kappa|)$. This increases the kinetic energy independent whether the interaction is attractive ($\nu < 1/2$) or repulsive ($\nu > 1/2$): $t > t_{\rm HF}$ as can be seen in Fig. 3. We note that n_κ has no discontinuity at $|\kappa| = 1$. Its value is $1/2$ and near $\kappa = 1$ it follows a power law as is typical for all Luttinger liquids with their $z_{\rm F} = 0$ [44,45].

This thawing or melting of the Fermi ice block (which accompanies the above discussed broadening/narrowing of the PD) we model analytically with the continuous function

$$
n_\kappa = \frac{1}{2} + B(1-\kappa)^\beta \left[1 + b_1^-(1-\kappa)^\beta + b_2^-(1-\kappa)^{2\beta} + \ldots\right] \quad \text{for } 0 \leq \kappa \leq 1, \tag{28a}
$$

$$
n_\kappa = \frac{1}{2} - B(\kappa-1)^\beta \left[1 + b_1^+(\kappa-1)^\beta + b_2^+(\kappa-1)^{2\beta} + \ldots\right] \quad \text{for } 1 \leq \kappa \leq 2, \tag{28b}
$$

$$
n_\kappa = \frac{C}{\kappa^\gamma}\left(1 + \frac{c_2}{\kappa^2} + \frac{c_4}{\kappa^4} + \ldots\right) \quad \text{for } 2 \leq \kappa \leq \infty \tag{28c}
$$

with [24,46]

$$
\beta = \frac{1}{4}\frac{(1-2\nu)^2}{1+2\nu} \tag{29}
$$

and $\gamma = 3 + 2\nu$ (Appendix B). The exponents β, γ and the coefficients B, C, and $b_i^\pm, c_i$ depend on ν. It should be $\beta < 1$. Eqns. (28b) and (28c) describe the correlation tail ($\kappa > 1$). This n_κ has to obey the normalization (17) and the condition

$$
3\int_0^\infty d\kappa\ n_\kappa \kappa^2 = \frac{\left(\frac{1}{2}+\nu\right)^2}{2\nu} \geq 1\ , \tag{30}
$$

which follows from Eq. (18) together with the Hellmann-Feynman theorem (11). For $\nu = 1/2$ (or HF) it is $\beta = 0$, $B(1 + \sum_i b_i^\pm) = \frac{1}{2}$, and $C = 0$. The correlation induced melting for $\nu \neq 1/2$ shows up in $\beta > 0$, $B(1+\sum_i b_i^\pm) < \frac{1}{2}$, and $C > 0$.

C. Results of the exact solution

With the help of the Bethe-Ansatz technique one obtains [23,24] $e = \lambda^2 e_0$. e as a function of the interaction strength parameter λ shows no special behavior for $\lambda \underset{\to}{>} 1/2$, but as a function of the interaction strength $\mu = \lambda(\lambda - 1)$,

$$
e = \left(\frac{1}{2} + \nu\right)^2 e_0, \quad \nu = \sqrt{\frac{1}{4} + \mu} \tag{31}
$$

the non-analytical behavior for $\mu \to -1/4$ is incorporated in the variable ν. For $\nu \to 1/2$ it behaves like $e \to (1 + 2\mu)e_0$.

Eq. (31) yields with the Hellmann-Feynman theorem (13) the kinetic energy per particle,

$$
t = \frac{\left(\frac{1}{2}+\nu\right)^2}{2\nu} e_0 \tag{32}
$$

which behaves for $\nu \approx 1/2$ like $t \approx (1 + 5\mu^2)e_0$ in agreement with the above qualitative discussion as shown in Fig. 3. Eq. (31) yields with Eq. (12) also the interaction energy per particle

$$
v = \mu\left(1 + \frac{1}{2\nu}\right)e_0 \tag{33}
$$

which behaves for $\nu \approx 1/2$ like $v = 2\mu$ again in agreement with the above qualitative discussion. From Fig. 3 we see that both t and v diverge for $\nu \to 0$, while e remains finite.

Eqns. (32) and (33) lead to

$$
\int_0^\infty d\kappa\ n_\kappa \kappa^2 = 6\nu\left[\int_0^\infty \frac{dy}{\pi}\ \frac{g(y)}{y^2}\right]^2, \tag{34}
$$

as another integral relation between the momentum distribution n_κ and the dimensionless PD $g(y)$ in addition to Eq. (21). These distribution functions have to change with ν in such a way that these relations (21) and (34) are obeyed together with the normalization conditions (17) and (19).

The PD $n(x_{12}) = n^2 g(y)$ with $y = k_{\rm F}x_{12}$ is known analytically for the values $\nu = 0,\ 1/2$, and $3/2$ [23,24]. For $\nu = 0$ it is (with the notation of Appendix A)

$$
g(y) = 1 - \left(\frac{\sin y}{y}\right)^2 + \mathrm{Si}(y)\frac{d}{dy}\frac{\sin y}{y} - \frac{\pi}{2}\frac{d}{dy}\frac{\sin y}{y}, \tag{35}
$$

for $\nu = 1/2$ (ideal Fermi gas) it is

$$
g(y) = 1 - \left(\frac{\sin y}{y}\right)^2, \tag{36}
$$

and for $\nu = 3/2$ it is

$$g(y) = 1 - \left(\frac{\sin 2y}{2y}\right)^2 + \mathrm{Si}(2y)\frac{d}{d(2y)}\frac{\sin 2y}{2y}. \quad (37)$$

The corresponding dimensionless cumulant PDs $h(y) = 1 - g(y)$ are given in Table II together with their Fourier transforms

$$\tilde{h}(q) = 2\int_0^\infty dy \cos(qy)\, h(y). \quad (38)$$

They have via $S(q) = 1 - \tilde{h}(q)/\pi$ a simple relation to the static structure factor (or van Hove correlation function) $S(q) = \langle \hat{\rho}_q \hat{\rho}_q^\dagger \rangle / N$, which describes the correlation of density-density fluctuations. $\hat{\rho}_q = \sum_i \exp(-\mathrm{i}qx_i)$ is the Fourier transform of the density operator $\hat{\rho}(x) = \sum_i \delta(x - x_i)$. The three PDs $g(y)$ are shown in Fig. 1 and the three structure factors $S(q)$ in Fig. 4.

For $\nu = 1/2$ the weak oscillations of $g(y)$ and the (first-order) kink of $S(q)$ arise from the Fermi momentum distribution n_κ with its sharp discontinuity $z_\mathrm{F} = 1$ at $\kappa = 1$. With increasing repulsion the oscillations of $g(y)$ are enhanced, what is displayed in the reciprocal space by the peak of $S(q)$ at $q = 2$ (and a 3rd-order kink at $q = 4$). The first maximum of $g(y)$ runs through a certain trajectory from $(\pi,\ 1)$ to $(2.99,\ 1.24)$. This is analog to the electron gas model (where the term Friedel oscillations is used and) which shows with increasing r_s (i) enhanced oscillations with corresponding trajectories of the maxima and minima [47] and (ii) the emergence of an increasing hump in $S(q)$ at $q = 2$ [48]. This hump structure is even more marked in the (approximately frequency independent) local field correction $G(q)$ which appears in the dynamic structure factor $S(q, \omega)$ [49–52], from which then follows the static structure factor via $S(q) = \int d\omega/(2\pi)\ S(q, \omega)$ [21]. One of the differences between the CS and the electron gas model is that in the latter case z_F continuously decreases with increasing r_s starting with $z_\mathrm{F} = 1$ for $r_s = 0$, whereas in the CS model there is no adiabatic continuity [45] and z_F abruptly jumps from 1 to zero when going from $\nu = 1/2$ to $\nu \neq 1/2$. Whereas repulsion enhances the Friedel oscillations of $g(y)$ and the kink structure of $S(q)$, increasing attraction let them disappear: for $\nu = 0$ both $g(y)$ and $S(q)$ approach the value 1 smoothly (non-oscillatory) from below. But the kink structure of $S(q)$ at $q = 2$ has a relict in this limit: the 2nd derivative is discontinuous (2nd-order kink). For the on-top behavior of $g(y)$ in terms of $g(0)$, $g'(0)$, $g''(0)$ the following holds: It is $g(0) = 0$, according to the Pauli principle, $g'(0) = \pi/6$ for $\nu = 0$, but 0 for $\nu > 0$, and it is $g''(0) = 0$ for $\nu = 0$, infinite for $0 < \nu < 1/2$, but $2/3$ for $\nu = 1/2$, and 0 for $\nu > 1/2$.

With the identities (A2)–(A4) the normalization condition (19) is fulfilled. From Eqns. (35)–(37) follow the on-top coefficients of Eq. (22); they are shown in Table I. Note that the last two terms of Eq. (35) do not contribute to the normalization because of Eq. (A3) and that the last term causes the odd on-top coefficients of Table I and also the linear behavior for small y. Its oscillations are exactly canceled by the combined oscillations of the second and the third term. Simultaneously, these terms ensure the correct normalization.

The PD (36) for $\nu \to 1/2$ plugged into Eq. (10b) yields with the identity (A5) the same as results from Eq. (33), which follows from the total energy per particle, Eq. (31), and the Hellmann-Feynman theorem (13), namely $v = 2\mu e_0$. Similarly the PD (37) for $\nu \to 3/2$ plugged into Eq. (20) yields with the identities (A5) and (A6) the same as results from Eq. (33), namely $v = 4\mu e_0/3$.

For $\nu = 0$ a divergence appears, because from the PD (35) follows an on-top behavior, which is linear in y as shown in Fig. 1 and Table I. This linear behavior results from the last term of Eq. (35), which does not influence the normalization (19), but it makes the interaction energy $v \sim \int_0^\infty dy\ g(y)/y^2$ to diverge logarithmically in agreement with the divergence of $v \to -e_0/8\nu$ for $\nu \overset{>}{\to} 0$ as displayed in Fig. 3.

The divergence of the interaction energy is accompanied and compensated by the corresponding divergence of the kinetic energy $t \to e_0/8\nu$. This indicates a special asymptotic behavior of the momentum distribution n_κ for $\nu \overset{>}{\to} 0$, namely Eq. (28c) with $\gamma \overset{>}{\to} 3$. For $\gamma > 3$ the integral $\int_0^\infty d\kappa\ n_\kappa \kappa^2$ is convergent, but with $\gamma \overset{>}{\to} 3$ for $\nu \overset{>}{\to} 0$ it diverges logarithmically, whereas the normalization integral (17) remains convergent. The counterpart to this asymptotic behavior of n_κ for $\kappa \to \infty$ is the on-top behavior of the PD for $y \to 0$ as shown in Fig. 1 and Table I with a smooth transition of the coefficient A in Eq. (22) from $\pi/6$ via $1/3$, to $16/135$ for $\nu = 0,\ 1/2$ and $3/2$, respectively. With quadratic interpolation of the coefficients shown in Table I as functions of ν, one may continuously switch the on-top behavior of the PD $g(y)$ between its form at $\nu = 0$ and $3/2$. For the PD exponent $\alpha = 1 + 2\nu$ we refer to Appendix B, where also the momentum-distribution exponent is conjectured as $\gamma = 3 + 2\nu$.

These divergences of the kinetic and the interaction energies indicate that for attractive particle interaction μ/x_{ij}^2 with $\mu \to -1/4$ the system becomes unstable (no ground state with finite kinetic and potential energies). We remark that it was shown in Ref. [38] that the singular particle interaction $-|\mu|/|\vec{r}_{12}|^2$ makes already two particles to fall together ("fall-into-the-origin") for $|\mu| > 1/4$ (ground state with $E \to -\infty$) and for $|\mu| < 1/4$ there are only scattering states with $E \geq 0$ (no bound states with $E < 0$) [23].

For $\nu = 0$ the exact solution of the CS model yields the momentum-distribution data. In Section VI we will give the details of the necessary numerical calculation. The coefficients of Eq. (28a) are fitted to the n_κ values for $\kappa = 0 \dots 1$ and the coefficients of Eq. (28b) are fitted to the n_κ values for $\kappa = 1 \dots 2$. The coefficients are chosen to make also n_κ at $\kappa = 2$ continuous and smooth. Finally b_3^+ is fine tuned to make the normalization equal to 1 according to (17). The results are shown in Fig. 2 and the values of the coefficients are given in Table IV. The case $\nu = 3/2$ is similarly treated only with the difference that also the kinetic energy $t = \frac{4}{3}e_0$ can be used for the fine tuning in addition to the normalization condition (17). The results are shown also in Table IV. Here b_3^+ and b_4^+ have been used for fine tuning (which yields the normalization 0.997 and $t = 1.34\ e_0$, instead of 1 and $4e_0/3$).

V. FLUCTUATION-CORRELATION ANALYSIS

A. Quantities following from the pair density

Particle-number fluctuations: Following Fulde [1] one may ask to what extent correlation influences particle-number fluctuations ΔN_X in a domain X, *i.e.*, a certain interval of the x axis, where in the average there are $N_X = nX$ particles. These fluctuations are measured quantitatively by [1,3,13]

$$\begin{aligned}\frac{(\Delta N_X)^2}{N_X} &= 1 - \frac{1}{nX}\int_0^X dx_1 \int_0^X dx_2\ w(x_{12}) \\ &= 1 - \frac{1}{Y}\int_0^Y dy_1 \int_0^Y dy_2\ \frac{h(y_{12})}{\pi},\end{aligned} \tag{39}$$

with $Y = k_F X = \pi n X$. Following the Appendix A of Ref. [3] the 2D integral (39) is reduced to a 1D integral with the help of the Fourier transform (38), namely

$$\frac{(\Delta N_X)^2}{N_X} = 1 - \frac{2}{Y}\int_0^\infty \frac{dq}{\pi}\frac{1-\cos(qY)}{q^2}\frac{\tilde{h}(q)}{\pi}. \tag{40}$$

The results are shown in Fig. 5, where also the case $\mu \to \infty$ ('strict' or 'perfect' correlation [3]) is displayed.

With $h(y) = 1 - g(y)$ and with the expansion of $g(y)$ according to Eq. (22) — see also the text after Eq. (37) — the small-X expansion of Eq. (39) is

$$\begin{aligned}\frac{(\Delta N_X)^2}{N_X} &= 1 + d_1 nX + d_2 (nX)^2 + d_3 (nX)^3 \\ &\quad + d_4 (nX)^4 + d_5 (nX)^5 + \dots \quad .\end{aligned} \tag{41}$$

The slope d_1 at $X = 0$ does not depend on the interaction strength parameter ν as shown in Table III because of $g(0) = 0$ and $h(0) = 1$ not depending on ν; but the coefficients of the next terms do. Correlation is seen in the change of the coefficients d_i for $\nu = 1/2$ to the coefficients for $\nu \neq 1/2$. Thus the particle-number fluctuations are suppressed due to repulsive particle interaction, but enhanced due to attractive particle interaction: correlation makes the particle-number distribution $P_X(N)$ more narrow for repulsion ($\nu > 1/2$) and more broad for attraction ($\nu < 1/2$). We remark, that fluctuation enhancement (induced by attractive interaction) generally may support/cause clusterings (*e.g.*, paramagnons prior the para-to-ferromagnetic phase transition). In our case this tendency shows up in the sudden "fall-into-the-origin" at $\nu = 0$. If one considers with $X = 1/n$ a Wigner-Seitz 'sphere' (with 'radius' $X/2$ and $N_X = 1$), then

$$\Sigma_1(\nu) = 1 - \frac{\chi(\nu)}{\chi(1/2)}, \quad \chi(\nu) = \frac{(\Delta N_X)^2}{N_X} \tag{42}$$

is a reasonable correlation measure based on particle-number fluctuations as we show in Fig. 6.

On-top behavior: The exponent α and the coefficients A, a_i of Eq. (22) describe the short-range or dynamical correlation, *i.e.*, the small-separation behavior of $g(y)$, see Table I. Cioslowski's correlation cage [8] is in our case simply the inter-particle-separation range $y = 0 \dots y_{\max}$ with $y_{\max}$ being that separation where the PD $g(y)$ has its first maximum $g_{\max} = g(y_{\max})$. For $\nu = 0, 1/2, 3/2$ the corresponding values are $y_{\max} = \infty$, π, 2.99 and $g_{\max}$= 1, 1, 1.24 [3]. One may ask to what extent the correlation cage contributes to the interaction energy and define

$$\Sigma_2(\nu) = 1 - \frac{V_{\rm cage}(\nu)}{V_{\rm cage}(1/2)}, V_{\rm cage}(\nu) = \frac{\int_0^{y_{\max}} dy\ g(y)/y^2}{\int_0^\infty dy\ g(y)/y^2} \le 1 \tag{43}$$

as an energetic correlation measure with $V_{\rm cage}(0) = 1$; the expression simplifies when using (23). Both Σ_1 and Σ_2 vanish for $\nu = 1/2$ as shown in Fig. 6.

B. Quantities following from the momentum distribution

Critical exponent: The critical or correlation exponent β of Eq. (29) can be computed from conformal field theory [24,46]. It describes (together with the coefficient B) the behavior of n_κ near $\kappa = 1$ according to Eqns. (28a) and (28b). For the three special values $\nu = 0, 1/2$ and $3/2$, this gives $1/4, 0$, and $1/4$, respectively. The exponent γ describes the decay of the correlation tail.

Non-idempotency and correlation 'entropy': The q-order non-idempotency is [12] $c(q) = 1 - \int_0^\infty d\kappa\ (n_\kappa)^q$. The derivative of $c(q)$ at $q = 1$ is $s \equiv c'(1)$ or

$$s(\nu) = -\int_0^\infty d\kappa\ n_\kappa \ln n_\kappa \ge 0 \tag{44}$$

to be referred to as correlation 'entropy' [12,13]. It has been plotted in Fig. 7.

Correlation tail properties: The relative number of particles (or holes) in the corresponding correlation tail is [12,13,53]

$$N_{\text{tail}}(\nu) = \int_1^{\infty} d\kappa\; n_\kappa = \int_0^1 d\kappa\; (1 - n_\kappa) < 1. \tag{45}$$

The contribution of the correlation tail to s is [13]

$$S_{\text{tail}}(\nu) = -\int_1^{\infty} d\kappa\; n_\kappa \ln n_\kappa < s(\nu). \tag{46}$$

In addition to these quantum-kinematic measures one may use [13]

$$T_{\text{tail}}(\nu) = \frac{\int_1^\infty d\kappa\; n_\kappa \kappa^2}{\int_0^\infty d\kappa\; n_\kappa \kappa^2} \le 1 \tag{47}$$

as another energetic measure with $T_{\text{tail}}(0) = 1$. Also these correlation measures vanish for $\nu = 1/2$ as shown in Fig. 8.

C. The correlation energy

For $e_{\text{corr}} = e - e_{\text{HF}}$ follows

$$e_{\text{corr}} = -\left(\nu - \frac{1}{2}\right)^2 e_0 \,. \tag{48}$$

Kinetic and interaction energy contribute $t_{\text{corr}} = -\frac{1}{2\nu} e_{\text{corr}}$ and $v_{\text{corr}} = \left(1 + \frac{1}{2\nu}\right) e_{\text{corr}}$, respectively, to e_{corr}. Their ν-dependence is shown in Fig. 9.

D. Comparison of the correlation measures

When comparing the computed correlation measures in Figs. 6, 7 and 8 it turns out that for small $|\nu - 1/2|$ the PD based measures $\Sigma_{1,2}$ of Eqns. (42) and (43) are proportional to $\nu - 1/2$ (which is $-e'_{\text{corr}}/(2e_0)$), whereas the n_κ based measures (44)–(47) behave like $(\nu - 1/2)^2$ (which is $-e_{\text{corr}}/e_0$). So the latter ones are not so sensitive as the first ones. With $s(\nu) = 0.5828|e_{\text{corr}}/e_0| + \ldots$ the Collins' conjecture $|e_{\text{corr}}| \sim s$ is confirmed at least for weak interaction. In this limit also N_{tail}, S_{tail} and T_{tail} are mutually proportional and their derivatives are proportional to Σ_1 and Σ_2.

We remark that the quantities $\chi(\nu)$, $V_{\text{cage}}(\nu)$, $N_{\text{tail}}(\nu)$, $S_{\text{tail}}(\nu)$, and $T_{\text{tail}}(\nu)$ are reference free, *i.e.*, they are defined without reference to the non-interacting case $\nu = 1/2$ — which in our case is simultaneously equivalent to the Hartree-Fock approximation. References appear in $\Sigma_{1,2}$ with $\chi(1/2)$ and $V_{\text{cage}}(1/2)$ and in $s(\nu)$ with $s(1/2) = 0$. Whereas this observation is important for quantum chemistry — as stressed by J. Cioslowski [8] — whenever multi configuration appears, it is less important in our case which is well described by single configuration.

VI. NUMERICAL DETERMINATION OF 1PDM AND $n(\kappa)$ FOR THE CS MODEL

As has been noted previously in Ref. [23], the square of the ground state wave function in the periodic CS model for the special values $\nu = 0,\ 1/2$, and $3/2$ may be recognized as being identical to the joint probability density function for the eigenvalues of matrices from Dyson's ensemble [26]. The interaction strength parameters $\nu = 0, 1/2$ and $3/2$ correspond to orthogonal, unitary, and symplectic ensembles, respectively. Results from the theory of random matrices then enable the calculation of various correlation functions [23]. In particular, the 1PDM can be expressed in terms of a determinant of an appropriate matrix $F^{(\nu)}_{pq}$ [24]. The size of this matrix is specified by the number of particles N to be $(N-1)^2$ for $\nu = 1/2$ and $3/2$ and $(N-1)^2/4$ for $\nu = 0$. Each element of $F^{(\nu)}_{pq}$ contains simple trigonometric 1D ($\nu = 1/2$ and $3/2$) or 2D ($\nu = 0$) integrals.

For some cases, most notably $\nu = 1/2$, the resulting determinant can be computed analytically and corresponding expressions have been given in Ref. [24]. For the other cases, we have evaluated the determinant numerically [24], using a subdivision of the system volume (periodicity length) according to $L/L_0 = 42, 402$, and 402 for $\nu = 0,\ 1/2$, and $3/2$, respectively. The particle number, odd due to periodicity of the wave function [24], varied from $N = 1$ to 401, corresponding to a variation in density n from nearly 0 to nearly 1. Taking the Fourier transform, we next compute the momentum distribution n_κ for all densities. In Fig. 10, we show results for one of the three special ν values.

Next, we apply the definitions of correlation measures and correlation energies as given in Sections III, IV, and V and study their density dependence. In Fig. 11 we show results for the entropy s and in Fig. 12 for the various energies as the density is varied. As *all* energies scale with n^2, these measures should be *density independent* when normalized with respect to e_0. However, we do in fact see a pronounced density dependence for $n \gtrsim 0.5/L_0$ and also for $n \lesssim 0.05/L_0$. This latter density dependence is simply due to the small particle numbers, thus a small size of $F^{(\nu)}_{pq}$ and consequently a limited resolution when computing the 1PDM at fixed L/L_0. The density dependence at large n values is more intricate to explain. The computation of the 1PDM by the connection with random matrix theory works for the *periodic* model. Thus there exists a Brioullin zone and the tail of n_κ for $|\kappa|$ outside this Brioullin zone is folded back into it. The tail of n_κ thus tends to be dominated by this effect for large n values as shown in Fig. 10. However, knowing that the correlation measures must be independent of density in the thermodynamic limit, we deduce their values by restricting us to these density regions where the independence holds. Then we apply the fit according to Eq. (28)

as explained in Section IV B. In Fig. 7 we indicate by error bars the small variation in the correlation entropy when using instead of n_κ as in Fig. 2 the n_κ as in Fig. 10. Similarly, the corresponding variations in $N_{\rm tail}$, $S_{\rm tail}$, and $T_{\rm tail}$ are within the symbol sizes.

VII. EXTENSION TO IMPENETRABLE BOSONS AND LATTICE GASES

As mentioned in the introduction, the CS model is also solvable for bosonic particle symmetry. The bosonic wave functions have to obey an additional boundary condition, namely they have to vanish for inter-particle separations $x_{ij} \to 0$ such that the resulting system consists of *impenetrable* or hard-core particles [23] with additional μ/x_{ij}^2 interaction. Both PD and 1PDM may be calculated as before. The PD is independent of statistics [23], thus the fermionic exchange hole agrees with the bosonic impenetrability hole and all quantities computed before based on the PD are the same in the bosonic and the fermionic case. For the 1PDM this is different, the momentum distribution of bosons is quite different from the fermionic n_κ as shown in Fig. 13. However, energetic quantities and correlation measures based upon those are nevertheless independent of the statistics and should thus be the same for bosons and fermions. In Fig. 12 we show that this is indeed the case. Thus besides the density independence we have another criteria that allows us to extract the correct values of the correlation measures from these plots. We note that the abovementioned unwanted density dependence is also present in the bosonic n_κ and visible in Figs. 11 and 12. Also present is the aliasing effect as shown in Fig. 14.

In Refs. [23,24], it had been shown to be useful to restrict the family of wave functions of the CS model for both bosonic and fermionic symmetry to a lattice such that the coordinates are integers $x_j = 1, 2, \ldots L$ [54–56]. Only the normalization constants of the wave functions change and the 1PDM can be computed much as before [23], replacing the integrals in $F_{pq}^{(\nu)}$ by appropriate sums [24]. Furthermore, the structure factor $S(q)$ is known exactly and therefore also the PD [24]. The resulting lattice gas has a particle-hole symmetry and thus we need to consider $n \leq 1/2L_0$ only. However, the density N/L now enters all expressions in a non-trivial way and the very useful density independence of the continuum model for the quantities considered here is no longer applicable. Nevertheless, the continuum model corresponds to the low-density limit of the discrete model. In Fig. 11, we show that this is indeed the case for, *e.g.*, the correlation entropy.

VIII. DISCUSSION AND CONCLUSIONS

Both the PD based and the n_κ based correlation measures (42)–(47) vanish for $\nu = 1/2$ (no interaction). But the first ones are more sensitive because of $\Sigma_{1,2} \sim \nu - 1/2$ near to the no-interaction point as shown in Fig. 6, while the second ones are $\sim (\nu - 1/2)^2$ like $e_{\rm corr}$ of Eq. (48) as shown in Figs. 7 and 8 and therefore cannot distinguish between attractive and repulsive interactions. In 1D the PD based measures (42) and (43) are identical for fermionic and (hard core) bosonic particles. The n_κ based measures (44)–(47) do not apply for bosonic particles, they are designed for fermionic particles only. Thus for correlation measures of bosonic particles, the measures considered in this work are either inapplicable or identical to their fermionic counterparts as for the PD based measures and $e_{\rm corr}$.

Whereas for repulsive particle interaction results well-known from other extended many-body systems are confirmed again — enhancement of the Friedel oscillations with maxima/minima trajectories, humps/peaks of the static structure factor developing from its non-interacting kink, suppression of particle-number fluctuations — we have found in the present work that for switching on attraction particle-number fluctuations are contrarily enhanced and that this is accompanied by a smoothening of the PD (the oscillations disappear) and of the static structure factor (the kink disappears) as well as by the appearance of a linear on-top behavior of the PD. The latter behavior results in a diverging interaction energy in the strong attraction limit although the total energy remains finite. In momentum space the Fermi ice block thaws for both cases and correlation tails develop. In the strong attraction limit the correlation tail becomes so long ranged that the kinetic energy diverges, thereby exactly compensating the divergence of the interaction energy. We have shown that these divergences can be derived from the exactly known energy as a function of the interaction strength with the help of the Hellmann-Feynman theorem (11). This theorem allows to calculate $t(\nu)$ and $v(\nu)$ from $e(\nu)$ and gives — in addition to their normalizations (17) and (19) — exact relations for n_κ and the PD as shown in Eqns. (18) and (20).

In summary, we have applied the Hellmann-Feynman theorem to the 1D quantum system of $1/x_{ij}^2$ interacting particles making extensive use of the exact solution available for the CS model. We have analyzed particle-number fluctuations and studied measures for the correlation strength based on the pair density and on the momentum distribution. Our results show that the qualitative terms 'weak and strong correlation' can not be captured quantitatively in a single index, but rather a variety of quantities must be employed [13].

ACKNOWLEDGMENTS

RAR gratefully acknowledges support by the Deutsche Forschungsgemeinschaft (SFB393) and the hospitality of the Max-Planck-Institut für Physik komplexer Systeme (Dresden) for an extended stay where much of this work was started. PZ thanks the Max-Planck-Institut für Physik komplexer Systeme and P. Fulde for supporting this work.

APPENDIX A: CERTAIN INTEGRALS

The following identities are valid with $\mathrm{Si}(x) = \int_0^x dy[\sin(y)/y]$:

$$\int_0^\infty \frac{dx}{\pi}\frac{\sin x}{x} = \frac{\mathrm{Si}(\infty)}{\pi} = \frac{1}{2} \quad , \tag{A1}$$

$$\int_0^\infty \frac{dx}{\pi}\left(\frac{\sin x}{x}\right)^2 = \frac{1}{2} \quad , \tag{A2}$$

$$\int_0^\infty \frac{dx}{\pi}\left[\mathrm{Si}(\infty) - \mathrm{Si}(x)\right]\frac{d}{dx}\frac{\sin x}{x} = 0 \quad , \tag{A3}$$

$$\int_0^\infty \frac{dx}{\pi}\mathrm{Si}(x)\frac{d}{dx}\frac{\sin x}{x} = -\frac{1}{2} \quad , \tag{A4}$$

$$\int_0^\infty \frac{dx}{\pi}\frac{1}{x^2}\left[1 - \left(\frac{\sin x}{x}\right)^2\right] = \frac{1}{3} \quad , \tag{A5}$$

$$\int_0^\infty \frac{dx}{\pi}\frac{1}{x^2}\mathrm{Si}(x)\frac{d}{dx}\frac{\sin x}{x} = -\frac{2}{9} \quad . \tag{A6}$$

Eqns. (A2) – (A4) determine the normalization of the PD's (35) – (37). Eqns. (A5) and (A6) determine the interaction energy v for the HF approximation and for $\nu = 3/2$. For the fluctuation analysis with Eqns. (39) and (40)

$$\frac{2}{\pi}\int_0^\infty dy \cos(qy)\left(\frac{\sin y}{y}\right)^2 = \left(1 - \frac{q}{2}\right)\theta(2-q) \quad , \tag{A7}$$

$$\frac{2}{\pi}\int_0^\infty dy \sin(qy)\,\mathrm{Si}(y)\frac{\sin y}{y} = -\frac{1}{2}\ln|1-q|\;\theta(2-q) \quad , \tag{A8}$$

$$\frac{2}{\pi}\int_0^\infty dy \cos(qy)\,\mathrm{Si}(y)\frac{d}{dy}\frac{\sin y}{y} = -\left[1 - \frac{q}{2} + \frac{q}{2}\ln|1-q|\right]\theta(2-q) \quad , \tag{A9}$$

$$\int_0^\infty dy \cos(qy)\frac{d}{dy}\frac{\sin y}{y} = -\left[1 - \frac{q}{2}\ln\left|\frac{1+q}{1-q}\right|\right] \quad , \tag{A10}$$

$$\frac{2}{\pi}\int_0^\infty dy \cos(qy)\frac{\sin y}{y}\frac{d^2}{dy^2}\frac{\sin y}{y} = \frac{1}{6}(q-2)\left(q^2 - q + 1\right)\theta(2-q) \quad , \tag{A11}$$

$$2\pi\int_0^Y dy_1\int_0^Y dy_2\left(\frac{\sin|y_1 - y_2|}{|y_1 - y_2|}\right)^2 = 2\int_0^2 dq\,\frac{1-\cos qY}{q^2}(1 - \frac{q}{2}) = 1 - \cos 2Y - 2Y\mathrm{Si}(2Y) + \int_0^{2Y} dz\,\frac{1-\cos z}{z} \quad . \tag{A12}$$

APPENDIX B: KIMBALL LIKE THEOREMS FOR $n(x_{12})$ AND n_κ

The small separation or on-top behavior of the PD $n(x_{12})$ is derived here similarly as Kimball found the cusp relation $dg(k_{\mathrm{F}}r)/dr|_{r=0} = g(0)/a_{\mathrm{B}}$ [or $g'(0) = \alpha r_s g(0), \alpha = (4/9\pi)^{1/3}$] for the pair correlation of the 3D uniform electron gas [57]. We remark that the general coalescing cusp theorem is due to Kato [58]. Let us consider two adjacent electrons with the center-of-mass and relative coordinates, $X = (x_1+x_2)/2$ and $x = x_1 - x_2$, respectively. Focusing on the x dependence the Schrödinger equation can be written as

$$\left[-\frac{d^2}{dx^2} + \frac{\lambda(\lambda-1)}{x^2}\right]\varphi(x)\tilde{\Phi}(X, x_3, \ldots) = (E - H')\varphi(x)\tilde{\Phi}(X, x_3, \ldots), \tag{B1}$$

where H' contains the remaining terms in the Hamiltonian. Note the missing factor 1/2 in the kinetic energy term because the mass there has to be replaced by the reduced mass of the electron pair ($m \to m/2$). Because $E - H'$ is non-singular as x approaches zero, it is unimportant for small x. To lowest order in x we therefore have $\varphi(x) = x^\lambda + \ldots$, from which immediately follows $n(x) \sim x^{2\lambda}$ for the PD, see Eq. (22). This can be concluded for $\lambda \neq 1$ also directly from the many-body wave function $\Phi \sim \Pi_{i<j}x_{ij}^\lambda$ [23] and for $\lambda = 1$ from Eq. (36).

A similar treatment of the asymptotic large κ behavior of the momentum distribution n_κ seems to lead in Eq. (28c) to the conclusion $\gamma = 2\lambda + 2$. This corresponds to $n_{\kappa\to\infty} \sim g(0)/\kappa^8$ for the 3D uniform electron gas [53,57,59]. Note that in this case the exponent of $1/\kappa$ (like the powers of y in the small-separation PD $g(y) = g(0) + \alpha r_s g(0)y + Cy^2 + \ldots$) does not depend on the interaction strength ϵ^2, only the coefficients $g(0)$ and C depend on $r_s \sim \epsilon^2$. Unlike that, in the CS model also the exponents α and γ are interaction strength dependent.

[1] P. Fulde, *Electron Correlations in Molecules and Solids*, Springer, Berlin (1995).
[2] F. Schautz, H.-J. Flad, and M. Dolg, Theor. Chem. Acc. **99**, 231 (1998) and references cited therein.
[3] P. Ziesche, J. Tao, M. Seidl, and J.P. Perdew, preprint mpi-pks/9902003 and Int. J. Quantum Chem. **77**, 819 (2000). Here it is shown how particle fluctuation is reduced by exchange in the ideal Fermi gas, and further reduced by Coulomb correlation in the interacting electron gas of 1, 2, or 3 dimensions.
[4] S. Kurth and J.P. Perdew, Int. J. Quantum Chem. **77**, 814 (2000).
[5] R.F.W. Bader, *Atoms in Molecules*, Clarendon, Oxford (1990).
[6] C. Aslangul, R. Constanciel, R. Daudel, and Ph. Kottis, Adv. Quantum Chem. **6**, 93 (1972) and references cited therein.
[7] J.F. Dobson, J. Chem. Phys. **94**, 4328 (1991).
[8] J. Cioslowski and G. Liu, J. Chem. Phys. **110**, 1882 (1999) and references cited therein.
[9] P.-O. Löwdin, Phys. Rev. **97**, 1474 (1955). Here it is asked for the meaning of $\mathrm{Tr}(\gamma - \gamma^2)$, which is in our notation $Nc(2)$, see Eq. (27).
[10] D. M. Collins, Z. Naturforsch. **48a**, 68 (1993); Acta Cryst. A**49**, 86 (1992).
[11] C. J. Ramirez, J. H. M. Pérez, R. P. Sagar, R. O. Esquivel, M. Hô, and V. H. Smith, Jr., Phys. Rev. A**58**, 3507 (1998) and references cited therein.
[12] P. Ziesche, O. Gunnarsson, W. John, and H. Beck, Phys. Rev. B**55**, 10270 (1997); P. Ziesche, V. H. Smith, Jr., M. Hô, S. P. Rudin, P. Gersdorf, and M. Taut, J. Chem. Phys. **110**, 6135 (1999); and references cited therein.
[13] P. Ziesche, preprint mpi-pks/200001001 and J. Mol. Structure (THEOCHEM), in press.
[14] R.F.W. Bader and M.E. Stephens, Chem. Phys. Lett. **26**, 445 (1974).
[15] A.D. Becke and N.E. Edgecombe, J. Chem. Phys. **92**, 5397 (1990); A. Savin, R. Nesper, S. Wengert, and T.F. Fässler, Angew. Chem. Int. Ed. Engl. **36**, 1808 (1997) and references cited therein. In H.-J. Flad, F. Schautz, Y. Wang, M. Dolg, and A. Savin, Eur. Phys. J. D**6**, 243 (1999) the bonding of small group 12 clusters is analyzed in terms of the 'electron localization function' concept. Similarly the bonding in solids has been studied by M. Kohout, namely in ionic solids (Thesis, University Stuttgart, 1999) and in cubic and hexagonal element structures and Sphalerite and Wurtzite structures (private communication).
[16] P. Ziesche, preprint mpi-pks/9809002 and in: *Electron Correlations and Material Properties*, A. Gonis, N. Kioussis, and M. Ciftan, eds., Plenum, New York (1999), p. 361.
[17] A. Szabo and N. S. Ostlund, *Modern Quantum Chemistry*, Mc Graw-Hill, New York, 1982.
[18] B. L. Hammond, W. A. Lester, Jr., P. J. Reynolds, *Monte Carlo Methods in Ab Initio Quantum Chemistry*, World Scientific, Singapore, 1994.
[19] D.A. Mazziotti, Phys. Rev. A**60**, 4396 (1999); M. Ehara, Chem. Phys. Lett. **305**, 483 (1999); C. Valdemoro, Adv. Quant. Chem. **31**, 37 (1999); and references cited therein.
[20] P. Fulde, H. Stoll, and K. Kladko, Chem. Phys. Lett. **299**, 481 (1999).
[21] P. Ziesche and G. Paasch, in: *Ergebnisse in der Elektronentheorie der Metalle*, P. Ziesche and G. Lehmann (eds.), Springer, Berlin, 1983, p. 14.
[22] G. Ortiz, M. Harris, and P. Ballone, PRL 82, 5317 (1999).
[23] B. Sutherland, J. Math. Phys. **12**, 246 (1971), B. Sutherland, J. Math. Phys. **12**, 251 (1971), B. Sutherland, Phys. Rev. A**4**, 2019 (1971), B. Sutherland, Phys. Rev. A**5**, 1372 (1972).
[24] B. Sutherland, Phys. Rev. B**45**, 907 (1992), R. A. Römer and B. Sutherland, Phys. Rev. B**48**, 6058 (1993).
[25] M. L. Mehta, *Random Matrices*, Academic Press, Boston, 1990.
[26] F. Dyson, J. Math. Phys. **3**, 140 (1962).
[27] A. M. Polyakov, Pis'ma Zh. Eksp. Teor. Fiz. **12**, 538 (1970), [JETP Lett. **12**, 381 (1970)].
[28] A. A. Belavin, A. M. Polyakov, and A. B. Zamolodchikov, Nucl. Phys. B **241**, 333 (1984).
[29] J. L. Cardy, Phys. Rev. Lett. **52**, 1575 (1984).
[30] J. L. Cardy, in *Phase Transitions and Critical Phenomena*, edited by C. Domb and J. L. Lebowitz, Academic, New York, 1987, Vol. 11.
[31] B. Sutherland and R. A. Römer, Phys. Rev. Lett. **71**, 2789 (1993).
[32] B. Sutherland, R. A. Römer, and B. S. Shastry, Phys. Rev. Lett. **73**, 2154 (1994).
[33] B. D. Simons and B. L. Altshuler, Phys. Rev. Lett. **70**, 4063 (1993).
[34] B. D. Simons and B. L. Altshuler, Phys. Rev. B **48**, 5422 (1993).
[35] V. E. Kravtsov and A. M. Tsvelik, (2000), cond-mat/0002120.
[36] M. A. Olshanetsky and A. M. Perelomov, Phys. Rep. **71**, 313 (1981).
[37] H. Hellmann, *Einführung in die Quantenchemie*, Deuticke, Leipzig, 1937, pp. 61, 285 (the original russian version is of 23 October 1936: G. Gel'man, Quantenchemie, ONTI, Moscow and Leningrad, p. 428); R. P. Feynman, Phys. Rev. **56**, 340 (1939); what usually is referred to as Hellmann-Feynman theorem has been first formulated by P. Güttinger, Z. Phys. **73**, 169 (1932), see his Eq. (11). This result is implicitly contained in Eq. (28) of M. Born and V. Fock, Z. Phys. **51**, 165 (1928). Whereas in these papers any parameter is considered, Hellmann and later Feynman explicitly referred to the special case of nuclear coordinates within the Born-Oppenheimer approximation, leading to the 'Hellmann-Feynman' forces upon nuclei. Within perturbation theory the theorem was already given by E. Schrödinger, Ann. Phys. (Leipzig) [4], **80**, 437 (1926). Thus the theorem is due to Schrödinger, Born, Fock, Güttinger, Hellmann, and Feynman.
[38] L. D. Landau and E. M. Lifshitz, *Quantum Mechanics*, Pergamon, Oxford, 1977, §35.
[39] M. Taut, Phys. Rev. A**48**, 3561 (1993).
[40] M. Taut, J.Phys. A**27**, 1045 (1994).
[41] M. Taut, J.Phys. A**32**, 5509 (1999).
[42] W. Macke and P. Ziesche, Ann. Physik (Leipzig) **13**, 73 (1964).
[43] P. Ziesche, in: *Advances in Theory of Many-Electron Densities and Reduced Density Matrices*, J. Cioslowski, ed., Kluwer/Plenum, New York, 2000, in press.

[44] F. D. M. Haldane, J. Phys. C: Solid State Phys. **14**, 2585 (1981).
[45] H. J. Schulz, G. Cuniberti, P. Pieri, cond-mat/9807366.
[46] N. Kawakami and S.-K. Yang, Phys. Rev. Lett. **67**, 2493 (1991).
[47] K. Aravind, A. Holas, K. S. Singwi, Phys. Rev. B**25**, 561 (1982).
[48] A. Holas, P. K. Aravind, K. S. Singwi, Phys. Rev. B**20**, 4912 (1979).
[49] D. N. Tripathi and S. S. Mandal, Phys. Rev. B**16**, 231 (1977).
[50] J. T. Devreese, F. Brosens, L. F. Lemmens, Phys. Rev. B**21**, 1349, 1363 (1980).
[51] K. Utsumi and S. Ichimaru, Phys. Rev. A**26**, 603 (1982).
[52] E. Chancón and P. Tarazona, Phys. Rev. B**37**, 4013 (1988).
[53] Y. Takada and H. Yasuhara, Phys. Rev. B**44**, 7879 (1991).
[54] F. Gebhardt and D. Vollhardt, Phys. Rev. Lett. **59**, 1472 (1987).
[55] B. S. Shastry, Phys. Rev. Lett. **60**, 639 (1988).
[56] F. D. M. Haldane, Phys. Rev. Lett. **60**, 635 (1988).
[57] J.C. Kimball, J. Phys. A**8**, 1513 (1975), see also Refs. [53,59].
[58] T. Kato, Commun. Pure Appl. Math. **10**, 151 (1957); see also R. T. Pack and W. B. Brown, J. Chem. Phys. **45**, 556 (1966) and S. Y. Chang, E. R. Davidson, and G. Vincow, J. Chem. Phys. **52**, 1740 (1970).
[59] H. Yasuhara and Y. Kawazoe, Physica **85A**, 416 (1976).

TABLE I. On-top exponent and coefficients of the PD according to Eq. (22).

ν	0	1/2	3/2
α	1	2	4
A	$\frac{\pi}{6}$	$\frac{1}{3}$	$\frac{16}{135}$
a_1	0	0	0
a_2	$-\frac{1}{10}$	$-\frac{2}{15}$	$-\frac{8}{35}$
a_3	$\frac{2}{45\pi}$	0	0
a_4	$\frac{1}{280}$	$\frac{1}{105}$	$\frac{32}{1225}$
a_5	$-\frac{4}{1575\pi}$	0	0
a_6	$-\frac{1}{15120}$	$-\frac{2}{4725}$	$-\frac{2176}{1091475}$
a_7	$\frac{4}{55125\pi}$	0	0
a_8	$\frac{1}{1330560}$	$\frac{2}{155925}$	$\frac{125696}{1092566475}$

TABLE II. Dimensionless cumulant PD $h(y)$ and the structure factor $S(q)$ used for the computation of ΔN_X and $\Sigma_1(\nu)$ as in Eqns. (40) and (42).

ν	$h(y)$	$S(q) = 1 - \tilde{h}(q)/\pi$
0	$\left(\frac{\sin y}{y}\right)^2 - \left[\mathrm{Si}(y) - \frac{\pi}{2}\right] \frac{d}{dy} \frac{\sin y}{y}$	$\left[q - \frac{q}{2}\ln(1+q)\right]\theta(2-q)$
		$+\left[2 - \frac{q}{2}\ln\frac{q+1}{q-1}\right]\theta(q-2)$
$\frac{1}{2}$	$\left(\frac{\sin y}{y}\right)^2$	$\frac{q}{2}\theta(2-q) + \theta(q-2)$
$\frac{3}{2}$	$\left(\frac{\sin 2y}{2y}\right)^2 - \mathrm{Si}(2y)\frac{d}{d2y}\frac{\sin 2y}{2y}$	$\left[\frac{q}{4} - \frac{q}{8}\ln\left\|1 - \frac{q}{2}\right\|\right]\theta(4-q)$
		$+\theta(q-4)$

TABLE III. Coefficients of the small-X expansion of $\frac{(\Delta N_X)^2}{N_X}$ as in Eq. (41).

ν	0	1/2	3/2
d_1	-1	-1	-1
d_2	$\frac{\pi^2}{18}$	0	0
d_3	0	$\frac{\pi^2}{18}$	0
d_4	$-\frac{\pi^4}{600}$	0	0
d_5	0	$-\frac{2\pi^4}{675}$	$\frac{16\pi^4}{2025}$

TABLE IV. Coefficients as in Eq. (28) calculated from the numerically determined momentum distribution n_κ for $\nu = 0$ and $3/2$ (at $n = 1/2L_0$).

$\nu = 0$

$\kappa \in [0,1]$		$\kappa \in [1,2]$		$\kappa \in [2,\infty]$	
B	0.863355	B	0.863355	C	0.017788
b_1^-	-0.746775	b_1^+	-0.750439	c_2	5.972791
b_2^-	0.731357	b_2^+	0.747380		
b_3^-	-0.420828	b_3^+	-0.433779		
		b_4^+	0.009552		

$\nu = 3/2$

$\kappa \in [0,1]$		$\kappa \in [1,2]$		$\kappa \in [2,\infty]$	
B	0.552286	B	0.552286	C	1.46369
b_1^-	0.434380	b_1^+	1.467126	c_2	2.053966
b_2^-	-0.570516	b_2^+	-4.156361		
		b_3^+	4.180551		
		b_4^+	-1.606130		

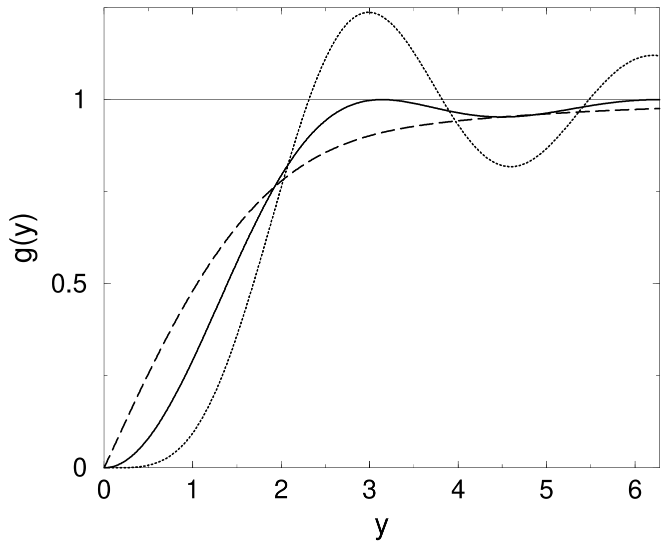

FIG. 1. Dimensionless PD $g(y) = n(x_{12})/n^2$ as a function of the dimensionless inter-particle separation $y = k_F x_{12}$ for $\nu = 0$ (dashed), 1/2 (solid), and 3/2 (dotted). The thin line is a guide to the eye only.

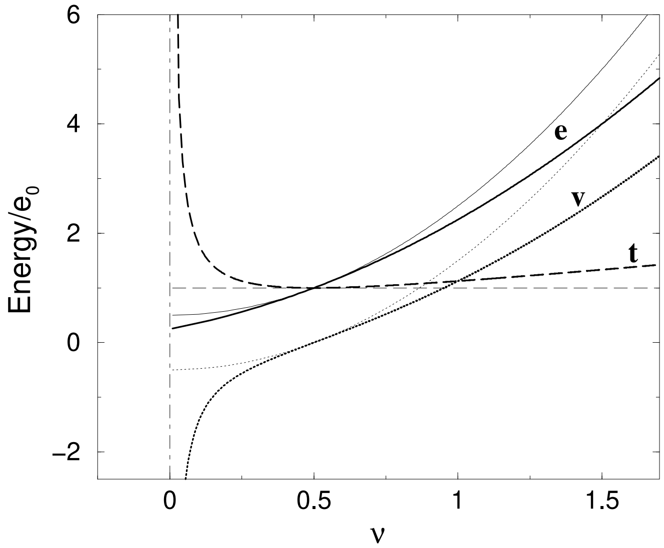

FIG. 3. Bulk energy e (solid), kinetic energy t (dashed), and potential energy v (dotted) plotted as functions of interaction strength parameter ν. Thin lines denote the results of the Hartree-Fock approximation, thick lines are exact. The thin dashed-dotted line indicates the "fall-into-the-origin" at $\nu = 0$.

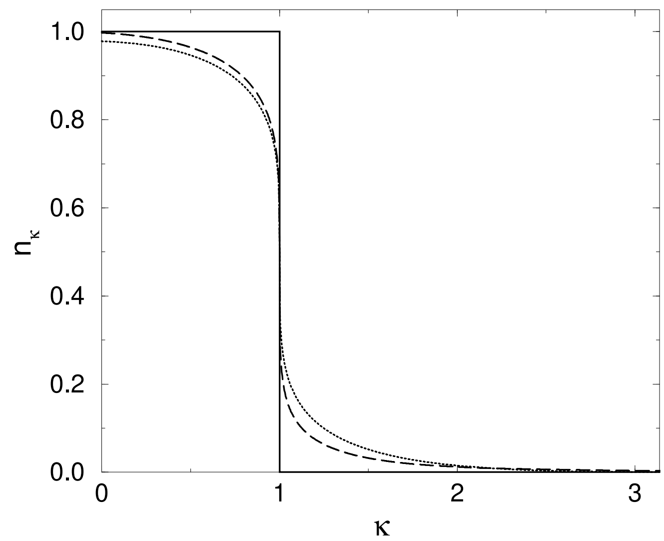

FIG. 2. Fermionic momentum distributions n_κ vs. $\kappa = k/k_{\mathrm{F}}$ with $\nu = 0$ (dashed), 1/2 (solid), and 3/2 (dotted).

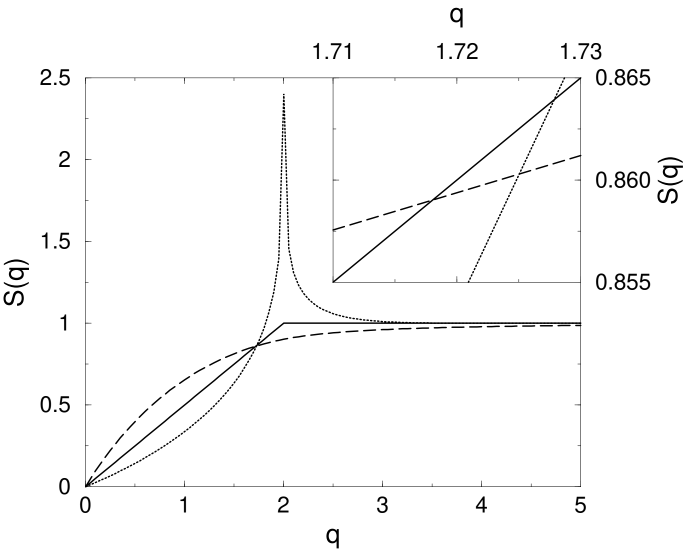

FIG. 4. Static structure factor $S(q) = 1 - \tilde{h}(q)/\pi$ for $\nu = 0$ (dashed), 1/2 (solid), and 3/2 (dotted). Inset: The three curves do not coincide at a single point close to $q \approx 1.72$.

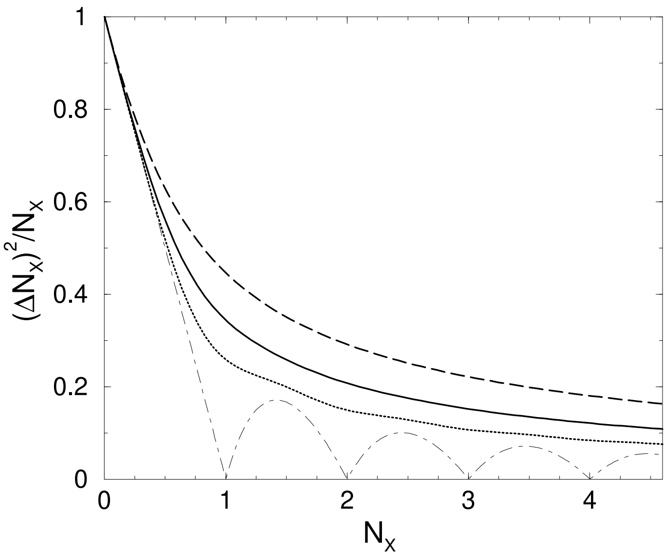

FIG. 5. Particle-number fluctuation $(\Delta N_X)^2/N_X$ in domains X of the CS model after Eq. (40) for $\nu = 0$ (dashed), 1/2 (solid), and 3/2 (dotted). The dashed-dotted line corresponds to $(\Delta N_X)^2/N_X$ for strict correlation [3].

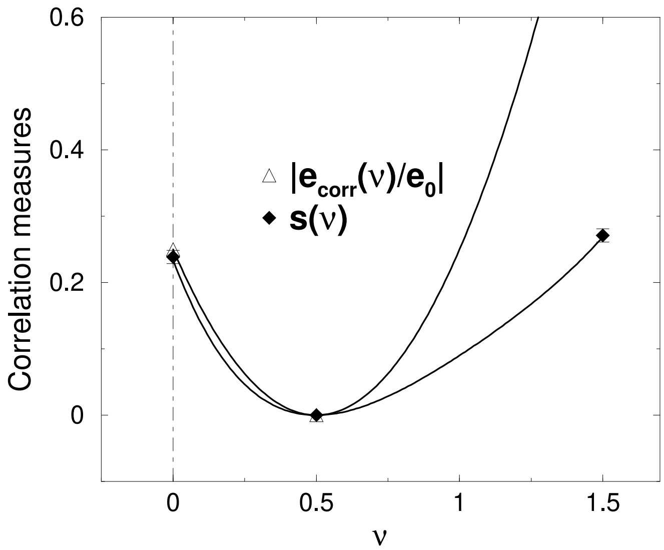

FIG. 7. Correlation 'entropy' s vs. ν as estimated from the fermionic momentum distributions according to Eq. (44) compared with $|e_{\rm corr}(\nu)/e_0|$ of Eq. (48). The solid lines are guides to the eye only. The thin dashed-dotted line is as in Fig. 6.

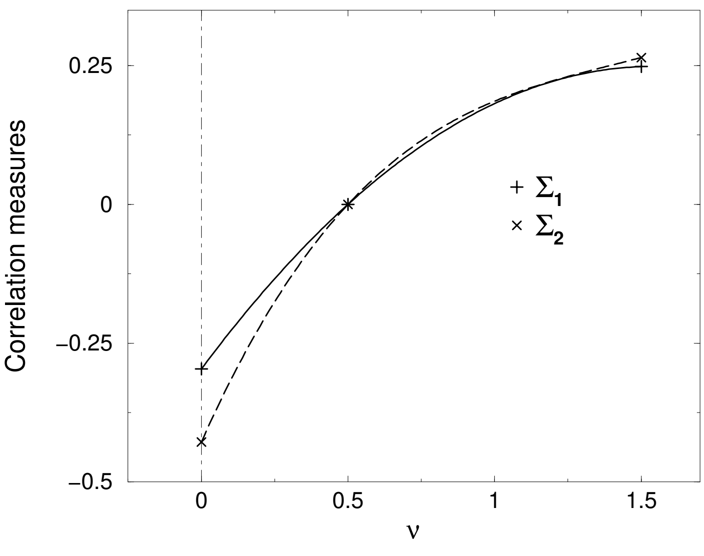

FIG. 6. PD based correlation measures $\Sigma_{1,2}$ according to (42) and (43) as functions of the interaction strength parameter ν. The thin dashed-dotted line indicates the "fall-into-the-origin" at $\nu = 0$. The other lines are guides to the eye only.

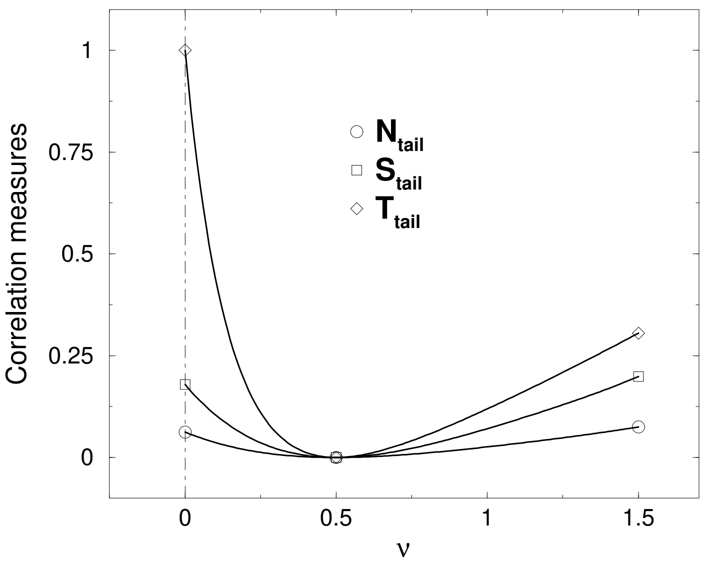

FIG. 8. Correlation measures based on the correlation tail of the momentum distribution according to (45) – (47) as functions of ν. The thin dashed-dotted line is as in Fig. 6. The other lines are guides to the eye only.

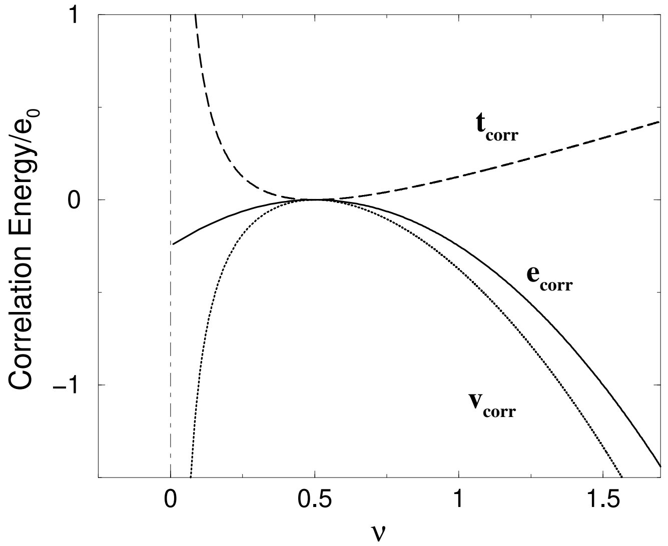

FIG. 9. Bulk (solid), kinetic (dashed), and potential (dotted) correlation energies as a function of ν. The thin dashed-dotted line is as in Fig. 3.

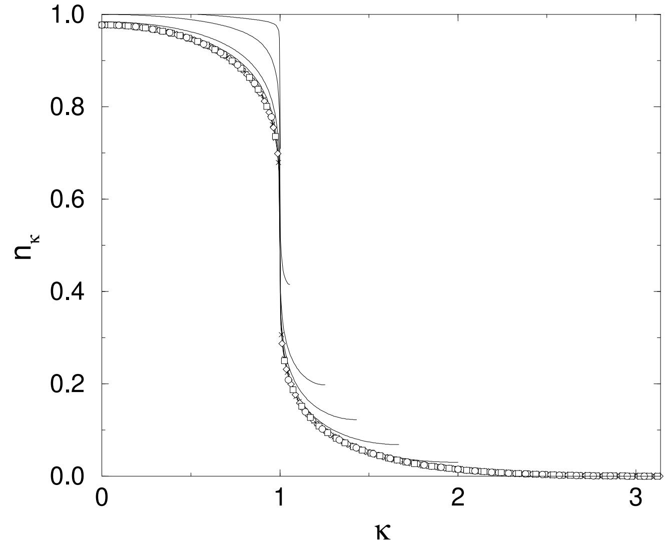

FIG. 10. Fermionic momentum distributions n_κ for $\nu = 3/2$ computed for $N = 21$, 41, 81, 121, 161, 201, 241, 281, 321, 361, and 401. The data for $N = 21(\circ)$, $41(\Box)$, $81(\diamond)$, and $121(\times)$ do not show any density dependence whereas the larger density data (lines) do.

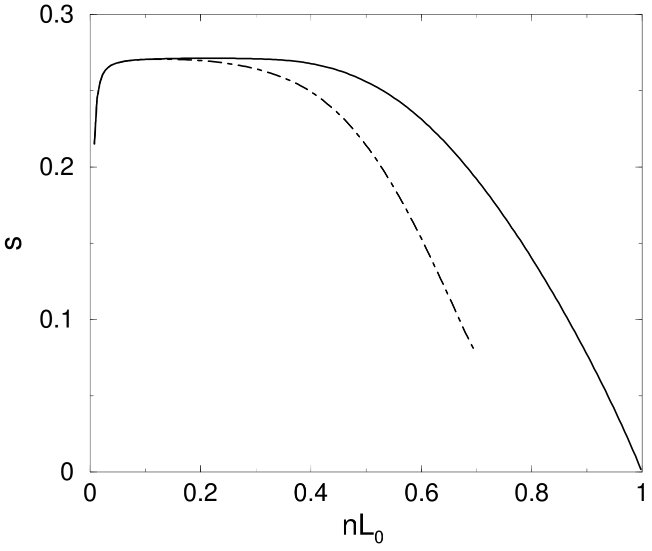

FIG. 11. Correlation 'entropy' (44) for fermions (solid line) as a function of density at $\nu = 3/2$. The dashed-dotted line corresponds to s obtained for the discrete CS model.

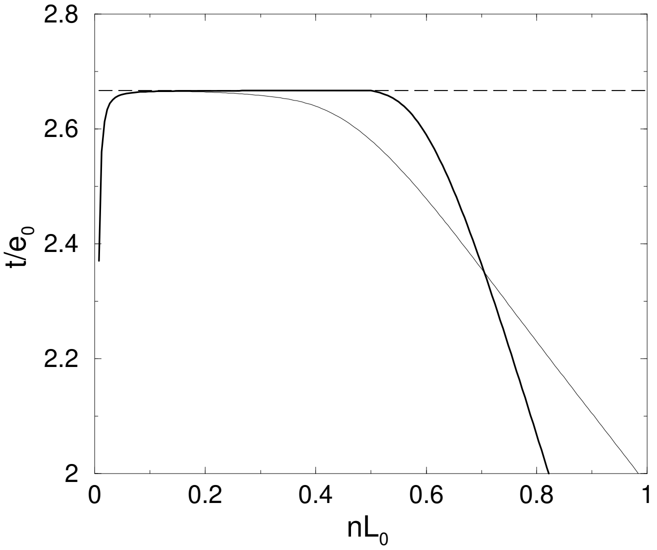

FIG. 12. Kinetic energy t as computed from the Hellman-Feynman theorem (11) (dashed line), and t from Eq. (13) (solid lines) for fermions (thick line) and bosons (thin line) as a function of density at $\nu = 3/2$.

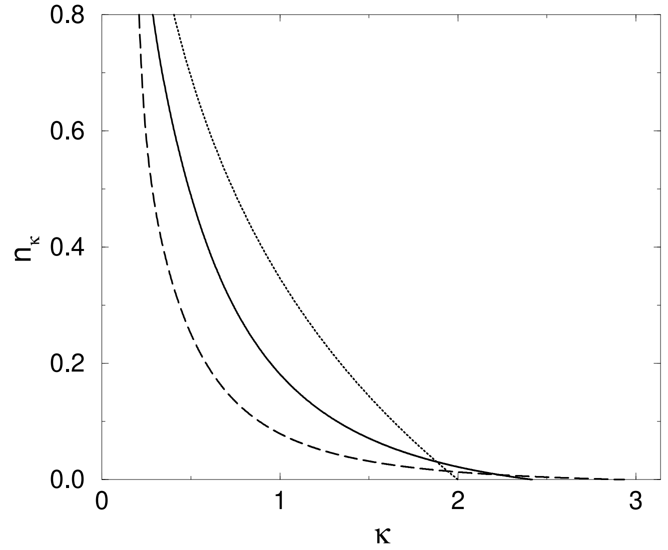

FIG. 13. Bosonic momentum distributions n_κ vs. $\kappa = k/k_{\mathrm{F}}$ with $\nu = 0$ (dashed), $1/2$ (solid), and $3/2$ (dotted).

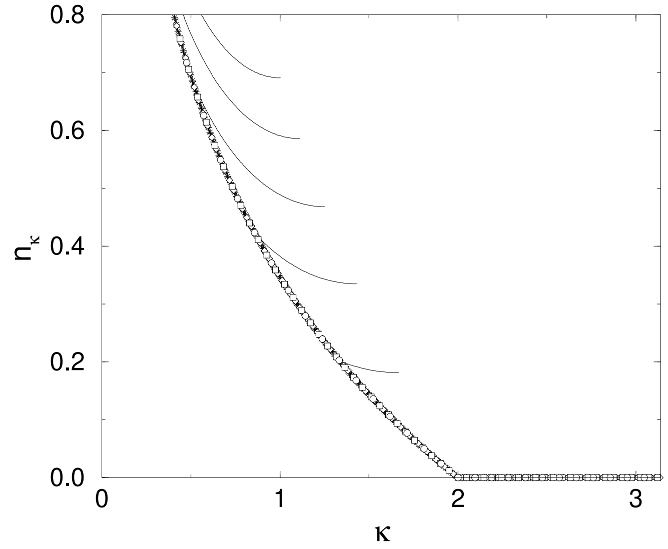

FIG. 14. Bosonic momentum distributions n_κ for $\nu = 3/2$ computed for particle numbers identical to Fig. 10. The data for $N = 21(\circ)$, $41(\Box)$, $81(\diamond)$, $121(\times)$, $161(+)$, and $201(*)$ do not show any density-dependence effects.